COLLECTIVE EFFECTS IN THE NSLS-II STORAGE RING*

S. Krinsky[#], J. Bengtsson, J.S. Berg, M. Blaskiewicz, A. Blednykh, W. Guo, N. Malitsky, C. Montag, B. Podobedov, J. Rose, N. Towne, L.H. Yu, BNL, Upton, NY, 11973-5000, U.S.A., F. Wang, MIT-Bates, Middleton, MA 01949

Abstract

A new high-brightness synchrotron light source (NSLS-II) is under design at BNL. The 3-GeV NSLS-II storage ring has a double-bend achromatic lattice with damping wigglers installed in zero-dispersion straights to reduce the emittance below 1nm. In this paper, we present an overview of the impact of collective effects upon the performance of the storage ring.   Subjects discussed include instability thresholds, Touschek lifetime and intrabeam scattering .

INTRODUCTION

In this paper, we discuss the effect of multi-particle interactions on the electron beam in the NSLS-II storage ring as described in the Conceptual Design Report [1]. The storage ring has 500 MHz RF and a revolution period of T_0=2.6 μs. The baseline design configuration corresponds to filling 80% of the RF buckets and leaving a 20% gap to allow for ion clearing. In this case we have M = 1040 bunches, each containing N_e = 7.8×10^9 electrons (N_ee = 1.25 nC) corresponding to a total average current I_{av}=MN_ee/T_0 =500 mA and a single-bunch current I_0=N_ee/T_0=0.5 mA. For an RMS bunch duration σ_t = 15 ps, the peak bunch current is I_p=N_ee/$\sqrt{2\pi}\,\sigma_t$ = 33 A.

The most accurate approach to estimating the instability thresholds for NSLS-II is to carry out computer simulation tracking studies using the wakefields determined by numerical calculation for each component comprising the storage ring. This large effort is now underway [2]. Here, we shall estimate instability thresholds using a simplified model of the ring impedance, which has been developed based on impedance calculations performed to-date and on the experience at existing storage rings [3], especially APS and ESRF. In addition to the wakefield effects mentioned above, we also discuss estimates of the Touschek lifetime resulting from single scattering, and of the increase in emittance due to multiple scattering.

We plan to use third-harmonic Landau cavities [4] to increase the bunch length and synchrotron tune spread. Lengthening the bunch raises the longitudinal microwave instability threshold, increases the Touschek lifetime and reduces the effect of intrabeam scattering on the emittance. Increasing the bunch length and synchrotron tune spread improves the effectiveness of positive chromaticity in raising the single and coupled bunch transverse instability thresholds.

INSTABILITY THRESHOLDS

We consider an approximate model of the storage ring impedance. The storage ring vacuum chamber is approximated by 720 m of aluminum with a vertical half-aperture of 12.5 mm. We also include 20 in-vacuum undulators, each with 3 m copper chambers of vertical half-aperture 2.5 mm. The geometric impedance due to cross-section changes in the vacuum vessel is approximated by longitudinal and transverse broadband resonators whose parameters are chosen based on experience at other storage rings [3] as well as on impedance calculations we have performed to-date. The impedance model is presented in Table 1, and some key beam parameters are given in Table 2. Calculations show [1] that radiation damping is sufficient to stabilize coupled bunch motion in the presence of the long-range wakefields due to the longitudinal and transverse higher-order modes in CESR-B superconducting cavities.

Table 1: Impedance Model

CESR-B HOMs	β_x=18m	β_y=3m	η=0

720 m of aluminum with half-gap of 12.5 mm and β_{av}= 7.6 m:
$$\kappa_\| = 4.0\,V/pC \quad \kappa_y = 0.68\,KV/pC/m$$

60 m of copper with half-gap of 2.5 mm and β_{av} = 2 m:
$$\kappa_\| = 1.3\,V/pC \quad \kappa_y = 5.6\,KV/pC/m$$

Transverse broadband impedance with f_r = 30 GHz, R_y = 1 MΩ/m, Q_y=1, and β_{av} = 7.6m : $\kappa_y = 19\,KV/pC/m$

Longitudinal broadband impedance with $f_r = 30GHz$, $R_s = 30k\Omega$, Q_s=1 : $(\mathrm{Im}Z_\|/n)_0 = 0.4\Omega \quad \kappa_\| = 35V/pC$

Table 2: Parameters for threshold calculations

Energy, E [GeV]	3
Revolution period, T_0 [μs]	2.6
Momentum compaction, α	3.7×10⁻⁴
Energy loss, U [keV]	1172
RF voltage, V [MV]	3.7
Synchrotron tune, ν_s	0.0094
Damping time: τ_x, τ_s [ms]	13, 6.5
Energy spread, $\sigma_{\varepsilon 0}$ [%]	0.09
Bunch duration, σ_{t0} [ps]	15

Transverse Mode Coupling Instability (TMCI)

An approximate relation [5] determining the threshold of the TMCI at zero chromaticity is given by

$$\frac{\Delta \nu_y}{\nu_s} = \frac{e I_0^{th}}{2 E \nu_s \omega_0} \sum_j \beta_{yj} \kappa_{yj} \cong 0.7 , \qquad (1)$$

where I_0^{th} is the threshold bunch current, β_{yj} is the average value of the vertical beta function in the jth element, and κ_{yj} is its kick factor. $E = \gamma mc^2$ is the electron energy and ν_s is the synchrotron tune. Consider a bunch current of 0.5 mA. Using the NSLS-II parameters as described in Table 2, we find that to be below the TMCI threshold requires

$$\sum_j \beta_{yj} \kappa_{yj} < 180 \ KV / pC . \qquad (2)$$

Using the values of the kick factors and beta functions as specified in Table 1, we find that $\sum_j \beta_{yj} \kappa_{yj} = 160 \ KV / pC$. Therefore, 0.5 mA bunches are below the TMCI threshold for zero chromaticity.

Longitudinal Microwave Instability

At very low single-bunch current, the longitudinal density is determined by the equilibrium between radiation damping and quantum fluctuations. As the bunch current increases, the longitudinal charge distribution is modified by the wakefield. Below the threshold of the microwave instability, the energy distribution remains unchanged, and the longitudinal charge distribution is determined by the time-independent solution of the Haissinski equation [6].

Once the current exceeds the microwave instability threshold, both the energy distribution and the charge distribution are modified and are no longer time-independent. In the case of a broadband resonator with shunt impedance R_s, resonant frequency ω_s, and quality factor $Q_s = 1$, Oide and Yokoya [7] have shown that the single-bunch current threshold is given by

$$I_0^{th} = \frac{E \nu_s \sigma_\varepsilon}{e R_s (\omega_r / \omega_0)} S(\omega_r \sigma_t) . \qquad (3)$$

From tracking studies using the program ELEGANT [8], we have found that in the regime x >0.2 a useful fit to the scaling function is given by

$$S(x) = 11 + 9.4 (x - 0.7)^2 . \qquad (4)$$

In Fig. 1, we show the dependence of the bunch length and the energy spread as calculated using the program ELEGANT [8]. This shows that 0.5 mA bunches will suffer negligible increase in energy spread due to the longitudinal microwave instability. These estimates we made without including the effect of a third-harmonic cavity. Including it will increase the microwave threshold.
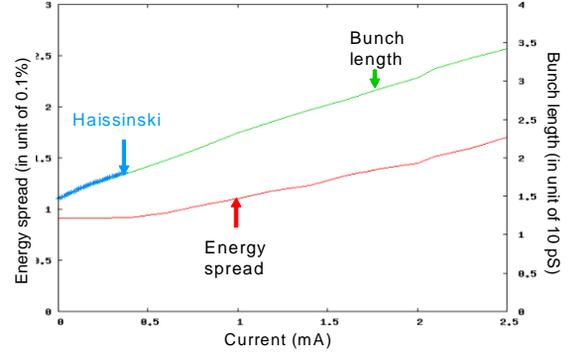

Figure 1: Bunch length and energy spread vs current

Transverse Coupled Bunch Instability

The short-range part of the resistive wall impedance contributes to the single-bunch TMCI. The long-range tail contributes to the transverse coupled bunch instability. Equating the growth time to the radiation damping time provides an estimate of the instability threshold. We find that the threshold is at a total average current of 15 mA, far below the design value of 500 mA. Running at positive chromaticity will increase this threshold value.

Particle tracking [9] has been used to estimate transverse stability thresholds for coupled bunch modes. In these calculations we include both the long-range and short-range resistive wall wakefields as well as the short-range longitudinal and transverse wakefields, as described in Table 1. To keep the problem manageable, we assume that all RF buckets contain identical bunches interacting via a single coupled bunch mode. A single bunch is tracked and the effect of other bunches is obtained by appropriate phase shifts under the assumption that the coherent frequency shift is small compared to the characteristic frequency width in the long-range transverse impedance. This should be an excellent approximation for the resistive wall impedance, which dominates the long-range transverse wake. The resistive wall impedance as well as the longitudinal and transverse broad band resonator parameters are as given in Table 1.

Three cases were simulated. Case 0 is a "stripped" case with no longitudinal wakes, no quadrupolar wakes (also referred to as detuning wakes), and no third-harmonic RF. Case 1 has the full suite of collective effects but no third harmonic cavity. Case 2 includes a perfect third harmonic cavity. The single-bunch threshold current as a function of vertical chromaticity is shown in Fig. 2. In cases 1 and 2, a chromaticity of 4 allows for an average bunch current of about 0.5 mA and hence for an average

stored current of 500 mA. This demonstrates the importance of running at positive chromaticity. Note also that bunch lengthening and enhanced synchrotron frequency spread introduced by the longitudinal wakefield and the third-harmonic cavity increase the effectiveness of positive chromaticity to stabilize the beam. Operating with large positive chromaticity can increase the instability threshold; however, it can reduce energy acceptance and shorten Touschek lifetime. Therefore, transverse feedback is included in the NSLS-II design.
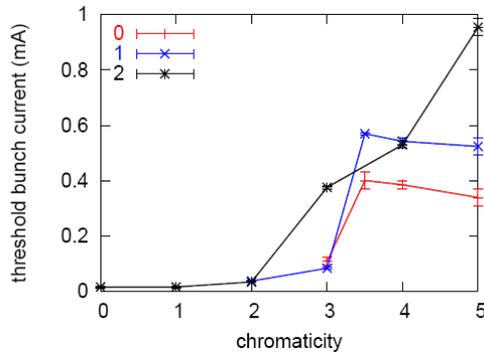

Figure 2: Threshold single bunch current vs. chromaticity for: (0) no longitudinal wakes, no quadrupolar wakes, and only fundamental RF; (1) all the impedances but only fundamental RF; (2) all impedances as well as fundamental and third-harmonic RF.

TOUSCHEK LIFETIME

NSLS-II operates in a regime where there is only a weak dependence of the Touschek lifetime on horizontal emittance. For small horizontal beamsize, the particle density of the bunch becomes large, increasing the probability of two electrons colliding. On the other hand, a small horizontal emittance results in small horizontal momentum that can be transferred into the longitudinal plane due to a Touschek scattering event. The Touschek lifetime vs emittance is plotted in Fig. 3, assuming a 3% energy acceptance.
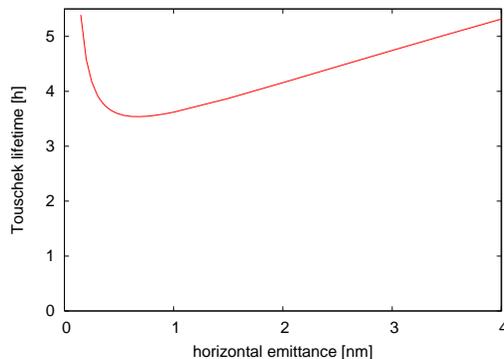

Figure 3: Touschek lifetime vs horizontal emittance.

Experience at facilities like ALS and SLS has shown that nonlinear betatron coupling plays a key role in limiting the momentum acceptance of the storage ring in the presence of small vertical apertures. Tracking performed using the TRACY-2 code demonstrates [10]

that with in-vacuum undulators having 5mm full-gap in the low-beta straights, a Touschek lifetime of 1.5 hrs can be achieved without third-harmonic cavity. A 3 hr lifetime can be achieved using third-harmonic RF.

INTRABEAM SCATTERING (IBS)

The NSLS-II emittance is strongly dominated by the IDs and damping wigglers. We have calculated IBS effects [11] as a function of radiation losses in the machine, having ε_{x0} vary from the ~2 nm bare lattice value down to about 0.4 nm. The zero-current vertical emittance ε_{y0} was fixed at the diffraction limit for 1 Å x-rays (8 pm-rad), corresponding to coupling varying from ~0.5% for bare lattice to about 2% for $\varepsilon_{x0} = 0.4$ nm.

Calculations have been performed with the code ZAP [12]. We assumed 500 mA average ring current uniformly distributed into 80% of the 500 MHz RF buckets. As we changed the amount of radiation losses, the RF voltage was adjusted to keep the RF energy acceptance constant at 3%. Electron beam parameters in the absence of IBS, used as input to ZAP (such as horizontal emittance, energy spread, bunch length, and radiation damping times) were calculated analytically by scaling bare lattice values by the amount of radiation losses. As the emittance w/o IBS is reduced, the damping time is also decreased. In Fig. 4, we see that IBS increases the horizontal emittance by ~20% for all values of the energy loss per turn. These estimates were done without harmonic RF. Adding it reduces the peak density and alleviates the IBS effect.
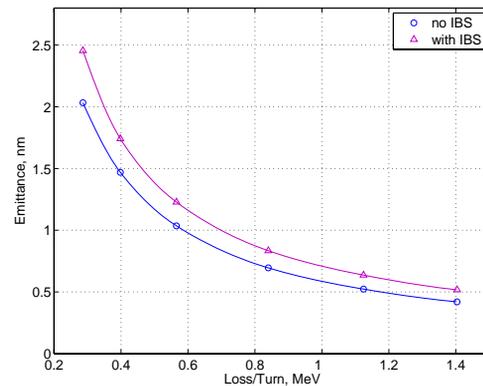

Figure 4: Emittance vs energy loss per turn

REFERENCES

[1] http://www.bnl.gov/nsls2/project/CDR/
[2] A. Blednykh and S. Krinsky, Proc. PAC 2007.
[3] K. Harkay et al., Proc. EPAC2002, 1505 (2002).
[4] A. Blednykh et al., Proc. PAC2005 (2005) 2544.
[5] See e.g., S. Krinsky, BNL-75019-2005-IR.
[6] J. Haissinski, *Il Nuovo Cimento* **18**, 72 (1973).
[7] K. Oide and K. Yokoya, KEK Preprint 90-10 (1990).
[8] M. Borland, http:// www. aps.anl.gov/Accelerator Systems Division/Operations Analysis/software.shtml
 [9] M. Blaskiewicz, Proc. PAC 2007.
[10] C. Montag and J. Bengtsson, Proc. PAC 2007.
[11] B. Podobedov, Proc. PAC 2007.
[12] M.S. Zisman et al, LBL-21270, UC-28 (1986).